Biotechnol. Bioprocess Eng. 2001, 6: 42-50

Rigorous Model for Spherical Cell-support Aggregate

Seung-Hyeon Moon[1]*, Ki Beom Lee[1], and Satish J. Paruekar[2]

[1] Department of Environmental Science and Engineering, Kwangju Institute of Science and Technology, Kwangju 500-712, Korea
[2] Department of Chemical and Environmental Engineering, Illinois Institute of Technology, Chicago, IL 60616-3793, USA

Abstract The activity of immobilized cell-support particle aggregates is influenced by physical and biochemical elements, mass transfer, and physiology. Accordingly, the mathematical model discussed in this study is capable of predicting the steady state and transient concentration profiles of the cell mass and substrate, plus the effects of the substrate and product inhibition in an immobilized cell-support aggregate. The overall mathematical model is comprised of material balance equations for the cell mass, major carbon source, dissolved oxygen, and non-biomass products in a bulk suspension along with a single particle model. A smaller bead size and higher substrate concentration at the surface of the particle, resulted in a higher supply of the substrate into the aggregate and consequently a higher biocatalyst activity.

Keywords: mathematical model, immobilized cell, material balance, bead size, biocatalysts

INTRODUCTION

The key physical and biochemical characteristics of gels have been widely investigated. These physical and biochemical characteristics significantly influence the activity of immobilized cell-support particle aggregates. Other factors affecting the activity of immobilized cells include mass transfer and the microbial physiology. The resistance to a mass transfer of nutrients and products can be reduced by reducing the particle size. However, the preparation and handling of particles is much more difficult. Therefore, the proper particle size should be selected based on the physical and biochemical properties of the immobilized cell-support particle aggregate, such as the effective diffusivity, consumption rate of the limiting substrate, maximum cell concentration, and the substrate concentration at the surface of the aggregate.

This paper presents a mathematical model for a spherical immobilized cell-support particle aggregate.

BACKGROUND

The effects of mass transfer have been incorporated in detail in models developed for chemical catalysis. The mathematical representation of immobilized cells has relied heavily on mathematical models used for chemical catalytic reactors. While the considerably richer knowledge base available for chemical reactors using supported catalysts can be fruitfully employed in developing a knowledge base for immobilized cell reactors, the significant differences in the functioning of chemical catalysts and biological catalysts (cells) must be recognized when attempting mathematical representations for the latter reactor type. The situation with immobilized cells is much more complex than that with chemical catalysts due to (i) continual cell growth and lysis and the leakage of cells, plus (ii) the non-uniform distribution of cells (and hence the spatial variations in the effective diffusivities of all diffusible species) in the support particles. Various models of immobilized cells (or enzymes) have been developed earlier and reported in previous studies.

With a few exceptions [1-4], the mathematical models for immobilized cell processes have been based on the assumption of uniform cell loading and uniform diffusivity in the support particles [5].

The steady state profiles of cell mass concentrations have been found to be highly non-uniform with a significant accumulation of cell mass occurring in the outer core of the support particle in many experimental studies [6,7]. Accordingly, it is evident that the predictions of mathematical models based on an assumption of uniform biomass activity in the support particle will be erroneous.

Even in mathematical models considering a non-uniform distribution of cell mass, the non-uniformity only occurs during a transient period. Therefore, in some of these models a steady state should not exist [4]. The model proposed in this study is capable of predicting a non-uniform distribution of cell mass in both

*Corresponding author
Tel: +82-62-970-2435 Fax: +82-62-970-2434
e-mail: shmoon@kjist.ac.kr

steady state and transient situations. A non-uniform cell mass distribution influences biochemical properties, such as the specific cell growth rate and effective diffusivities of the nutrients and products. The specific growth rate of immobilized cells is affected by the cell mass concentration since cell growth is inhibited by cell-cell contact or a reduction in the free volume available for cell growth. Cell mass inhibition kinetics have been employed for high cell density cultures and cell agglomerates [8]. Two types of cell mass inhibition growth kinetics have been used previously; Contois' equation [9] and a logistic equation [10].

$$\mu = \frac{\mu_X S}{K_X X + S} \tag{1}$$

$$\mu = \mu_{free}\left(1 - \frac{X}{X_m}\right) \tag{2}$$

Contois' growth kinetics, Eq. (1), employed for the analysis of agglomerate cells [11], does not predict the termination of cell growth at a finite mass concentration. The logistic equation, Eq. (2), appears to be a more realistic expression for describing the growth of immobilized cells with X_m being the maximum permissible cell density (determined by the space available in the immobilized cell-support aggregate). In Eq. (2), μ_{free} is the specific cell growth rate in the suspension culture. The maximum permissible cell mass concentration, X_m depends on the microorganism and immobilization conditions.

The effective diffusivities of substrates and products are also affected by the cell mass concentration owing to a change in the free volume. Theoretical and empirical expressions of diffusivities as a function of the cell mass concentration and polymer content have been suggested by previous investigators [12,13]. Zhao and DeLancey [13] employed a theoretical expression for effective diffusivity in a gel bead based on an analogy between the effective diffusivity in cell-laden gels and the effective thermal conductivity for composite materials.

$$\frac{D_e}{D} = \frac{\frac{2}{D_c} + \frac{1}{D} - 2\phi_c\left(\frac{1}{D_c} - \frac{1}{D}\right)}{\frac{2}{D_c} + \frac{1}{D} + \phi_c\left(\frac{1}{D_c} - \frac{1}{D}\right)} \tag{3}$$

where D, D_c, and ϕ_c are the molecular diffusivity of a species, its diffusivity through the cell, and the cell volume fraction, respectively. In this equation, the diffusivity of a substrate through the cells remains to be determined experimentally. For example the effective diffusivity of oxygen through *Candida utilis* cells was estimated to be around 40% of its molecular diffusivity in water [14].

A selection of reliable kinetic equations is an important element in the development of a mathematical model for an immobilized cell reactor. Special consideration should be given to rate-limiting substrates in cell growth and product-formation kinetics. In suspension cultures, kinetic studies are usually focused on the utilization of major carbon sources or other nutrients. In aerobic cell cultures within cell-support aggregates, the mass transfer resistance often leads to oxygen limitation as well as a carbon source limitation. Therefore, the specific cell growth and production rates decrease due to the mass transfer resistance of oxygen and/or other nutrients.

Chen and Humphrey [15] estimated the critical particle diameter for the transport of the oxygen of immobilized cells based on the assumption that immobilized cell beads have a uniform cell density and uniform diffusivities. Even though the effect of oxygen on cell physiology is more complicated, the effects of oxygen on microbial cell growth and metabolite production are similar to those of other nutrients. For example, the relationship between the oxygen concentration and the cell growth rate has been found to be Monod type [16,17]. In this regard, cell growth and product formation rates should be expressed in terms of the concentrations of multiple substrates [17].

THEORY

Unsteady State Equations

The complex metabolism of a living cell encompasses many reactions with multiple nutrients and products. While it is not possible to consider all these reactions within a mathematical framework, key reactions (in their absolute or lumped form) that at least describe processes such as cell growth, oxygen utilization, substrate consumption, and the formation of certain non-biomass products of interest must be incorporated.

As such, the single particle model (diffusion-reaction model) is comprised of a set of partial differential equations with the diffusion term for diffusible species absent from the material balance for the cell mass. Each diffusion equation requires two boundary conditions. In addition to the zero gradient boundary condition at the center of the particle, a Dirichlet or Robin boundary condition based on the flux balance for each species must be specified at the interface between the bulk liquid (bulk cell-liquid suspension to be exact) and the particle.

The function of porous support is the formation of a structure which inhibits cell movement. While a solid chemical catalyst provides a solid surface for catalytic reactions, the support used for cell entrapment provides a pore volume in which the cells are confined and cellular processes occur. The rates of both these processes and the transport of diffusible species should therefore be based on the pore volume of the immobilized phase.

To illustrate the dynamic behavior of a cell-support particle aggregate, a diffusion-reaction model comprised of material balances for the cell mass and limiting sub-

strates is presented. The material balances for the cell mass, substrate, co-substrate (or oxygen), and desired metabolite in an immobilized cell-support particle aggregate are provided below:

$$\frac{\partial X}{\partial t} = (\mu - k)X \tag{4}$$

$$\frac{\partial S}{\partial t} = \frac{1}{\left(1-\frac{X}{\rho_X}\right)r^2}\frac{\partial}{\partial r}\left(r^2 D_S \frac{\partial S}{\partial r}\right) - \frac{\delta_S X}{\left(1-\frac{X}{\rho_X}\right)} \tag{5}$$

$$\frac{\partial P}{\partial t} = \frac{1}{\left(1-\frac{X}{\rho_X}\right)r^2}\frac{\partial}{\partial r}\left(r^2 D_P \frac{\partial P}{\partial r}\right) - \frac{\pi X}{\left(1-\frac{X}{\rho_X}\right)} \tag{6}$$

$$\frac{\partial G}{\partial t}\frac{1}{\left(1-\frac{X}{\rho_X}\right)r^2}\frac{\partial}{\partial r}\left(r^2 D_G \frac{\partial G}{\partial r}\right) - \frac{\delta_G X}{\left(1-\frac{X}{\rho_X}\right)} \tag{7}$$

The material balances presented above are subject to the following initial and boundary conditions.

$$X = X_0,\ S = P = G = 0 \text{ at } t = 0, \quad 0 \le r \le R \tag{8}$$

$$\frac{\partial S}{\partial r} = \frac{\partial P}{\partial r} = \frac{\partial G}{\partial r} = 0 \quad \text{at} \quad r = 0,\ t > 0 \tag{9}$$

$$S = S_0,\ P = P_0,\ G = G_0 \quad \text{at } r = R,\ t > 0 \tag{10}$$

In Eq. (4), κ reflects the combined specific rates of endogenous maintenance and cell death. Since the distribution of the cell mass and cell activity in the aggregate can be extremely non-uniform, variations in the effective diffusivities in the aggregate resulting from changes in the cell concentration relative to the radial position were considered.

Eq. (3) was used to estimate the effective diffusivities, that is, the ratio of the diffusivity of a species based on the cells to its diffusivity in the abiotic phase selected as 0.4. The expressions for μ, δ_S, and π describe their dependence on the cell mass (X), dissolved oxygen (G), and limiting nutrients (S) and product (P) concentrations.

Steady State Behavior

For the sake of simplicity, the example of a single substitute is considered here. In this case, the steady-state behavior of an immobilized cell-support aggregate requires a simultaneous solution for the balances of the cell mass and substrate. Each steady state solution is therefore identified as a solution of the following equations.

$$\mu(S,X) = k \quad \text{or} \quad X = 0 \tag{11}$$

$$\frac{1}{r^2}\frac{d}{dr}\left(r^2 D_S \frac{dS}{dr}\right) = \delta_S X \tag{12}$$

The conservation equation for a viable cell mass accounts for loss due to cell death/lysis (which has been neglected in previous studies with the exception of [2,3]). Cells in the central core of a support particle are more prone to lysis/death (owing to nutrient limitation) than those near the exterior of the particle. The material balance for the cell mass yields an explicit/ implicit relation between the concentration of the cell mass (non-diffusible species) and the concentration of a rate-limiting substrate (or diffusible species in general).

Two boundary conditions are required to solve Eq. (12). At the interface between the bulk liquid phase and the porous space in the support particle, the substrate concentration is subject to the boundary condition

$$S = S_0 \quad \text{at} \quad r = R \tag{13}$$

A zero-gradient condition applies at the center of the particle for the limiting substrate, *i.e.*,

$$\frac{dS}{dr} = 0 \quad \text{at} \quad r = 0 \tag{14}$$

When the bioreaction process rates are controlled by the diffusion rates of essential nutrients, the limiting substrate does not reach the center of the aggregate. As such, there is a central core in which the concentration of the limiting substrate is present at a level (S_c) at which cell growth is not permitted. Accordingly, the boundary condition (14) can be restated as [1,18].

$$\frac{dS}{dr} = 0, \ at \quad S = S_e \ \text{at} \quad r = R_e \tag{15}$$

where S_c is the critical substrate concentration at and below which the cells cannot grow, S_c being dependent on the cell growth kinetics ($\mu(S_c, X)$-k =0 at X =0).

In the present study this boundary value problem was solved numerically for the case of a non-uniform cell mass distribution and non-uniform diffusivity.

The simulations using the diffusion-reaction model, results of which are discussed next, were based on the following kinetic expressions.

$$\mu = \frac{\mu_m S}{K_S + S + S^2/K_I}\left(1-\frac{X}{X_m}\right) \tag{16}$$

$$\delta = \frac{\mu}{Y_{X/S}} + m_S \tag{17}$$

In consideration of the restricted free space in a support particle, the specific cell growth rate, in addition to being a function of the concentration of the limiting substrate, is considered to be a decreasing function of the cell mass concentration, see Eq. (2), with the specific rate being zero at or beyond the critical cell mass con-

centration (cell mass concentration at which the pores are completely plugged with the cell mass or the integrity of the support particle is questionable). The specific substrate consumption rate, Eq. (17), was assumed to be related to the specific cell growth rate.

To simulate the situation where cell growth may be inhibited by the major product, the following expression for the specific cell growth rate was used.

$$\mu = \frac{\mu_m S}{K_S + S + S^2/K_I}\left(1-\frac{X}{X_m}\right)\left(1-\frac{P}{P_m}\right) \quad (18)$$

P_m being the critical product concentration at and beyond which cell growth is not possible. In this case, a linear relation between the specific substrate consumption rate and the specific product formation rate was assumed.

The numerical values assigned to the various kinetic parameters in these simulations were used in Table 1. These values were chosen within the range of typical bacterial fermentations. The concentration of the product was expressed in an arbitrary unit.

SIMULATIONS

The boundary value problems, Eqs. (11)-(15), were solved using the DGEAR method for the numerical integration of the material balance equation, Eq. (12), along with the variational technique developed by McGinnis [19] for convergence to a steady state solution. The transient profiles were obtained by integrating Eqs. (4) and (5) using an explicit form of the finite difference equations.

The simulations using the diffusion-reaction model for an immobilized cell-support particle aggregate were subject to the environmentally elucidated effects of particle size, concentration of the limiting substrate at the surface of the aggregate, and inhibition kinetics on the concentration distribution of the cell mass, substrate, and product. Cell leakage, physical destruction of cell-support particle aggregates, and blockage of the free volume in the aggregates by dead cells were not considered in this study.

Transient Behavior of Cell-Support Particle Aggregate

The distribution of the cell mass concentration in the immobilized cell-support aggregate at different times is illustrated in Fig. 1. The initial viable cell concentration depends on the concentration of the cell mass in the inoculum used for the preparation of the aggregate and the gelation procedure. In the simulations, the initial cell mass concentration was set at 1 g/L. Fig. 1 shows that during the early stages of the fermentation (0-10 h), the cell mass concentration at the surface increased significantly, while the cell mass concentration in the interior of the aggregate (r/R < 0.8) increased very slowly due to the limitation of the substrate.

Table 1. Numerical values in simulation

k	0.02 h^{-1}	P_0	0.0 unit/mL,
P_X	200 g dry cell/L active (wet) cell,	μ_m	1.0 h^{-1}
		K_S	0.1 g/L
D_{S0}	0.014 cm^2/h	K_I	1000.0 g/L (variable),
D_{P0}	0.0024 cm^2/h	$Y_{X/S}$	0.25 g cell/g substrate
R	0.15 cm (variable)	m_s	0.001 g substrate/g cell/h
X_0	1.0 g/L	X_m	100 g dry cell/L
S_0	1.0 g/L (variable)	P_m	0.575 unit/mL (variable)

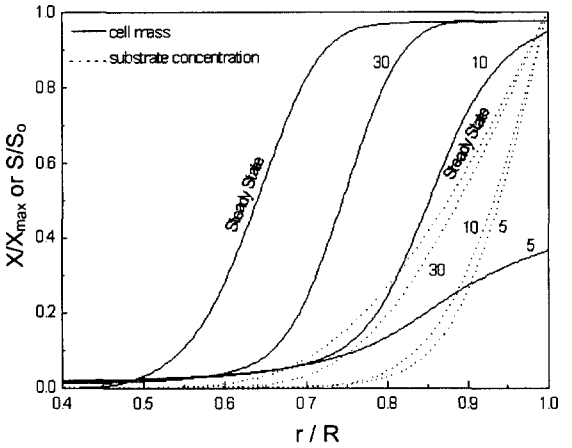

Fig. 1. Concentration profiles of cell mass and substrate. The numbers designate the fermentation time in h.

Once the cell mass concentration at the surface approached the maximum permissible cell concentration (X_m), the cell growth in the interior of the aggregate accelerated. The profiles approached a steady state after 100 h, at which point, the cell growth rate is equal to the cell death rate (including the endogenous metabolic consumption rate). For the parameter values considered here, the cell growth was restricted to the outer core beyond 50% of the bead radius. This trend of cell mass distribution is a typical example of an immobilized cell culture subject to a mass transfer limitation. The overall substrate consumption rates in the aggregate were 23.39, 12.50, and 7.08 in g/L free volume/h after 5 h, 10 h, and 30 h, respectively, and 6.54 g/L free volume/h in a steady state.

During the transient period a significant amount of substrate was consumed for cell growth, while in a steady state a lower amount of substrate was consumed for cell maintenance and product formation. In this example, the mass transfer resistance hampered the biocatalyst activity (the effectiveness factor based on the glucose consumption was 0.75 in a steady state). The following simulations present the steady state behavior of various bead sizes in immobilized cell-support particle aggregates.

Effects of Bead Size

The mass transfer resistance usually increases with an increased support particle size. The effect of the bead

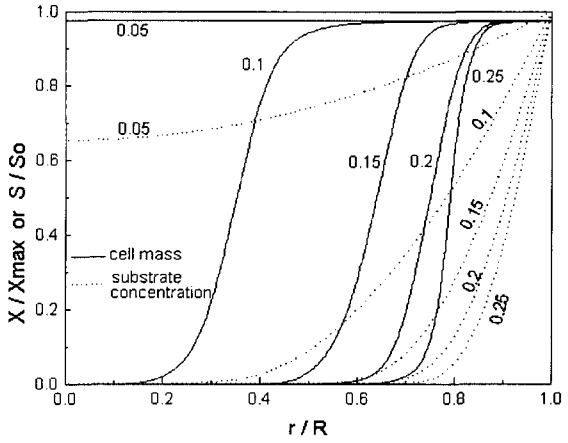

Fig. 2. Effect of particle size on steady state concentration profiles of cell mass and substrate. The numbers designate the particle radii in cm.

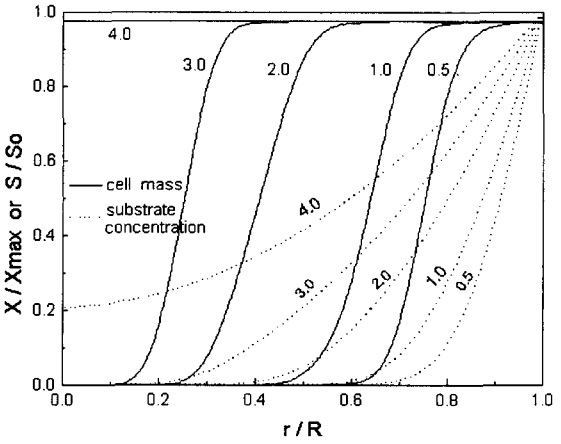

Fig. 3. Effect of substrate concentration at surface of immobilized cell-support particle aggregate on steady state concentration profiles of cell mass and substrate. The numbers designate the substrate concentration at the surface in g/L.

size on the distribution of the steady state cell mass and substrate concentrations is illustrated in Fig. 2. Bead sizes within a range of 0.1 to 0.5 cm in radius were considered. As the bead size increased, the volume fraction of the cell-free core also increased. The smaller beads exhibited higher average concentrations of cell mass and substrate.

The effectiveness factor was defined as the ratio of the glucose consumption rate in the aggregate to the glucose consumption rate at the surface. The effectiveness factors for immobilized cell particles 0.05 cm, 0.1 cm, 0.15 cm, 0.2 cm, and 0.25 cm in radius were 1.00, 0.95, 0.75, 0.61, and 0.50, respectively.

For the support particles with a radius of 0.05 cm, the cells and the substrate were distributed throughout the aggregate. Among the particle sizes investigated, the resistance to transport of the substrate was the least for those particles with a radius of 0.05 cm, hence the promotion of cell growth through the particles. The uniform cell density with a reduced bead size is preferable to maximize the biocatalyst activity. However, the preparation of small beads is more difficult and so is their confinement in the bioreactor. Doubling the particle size (from 0.05 cm to 0.1 cm in radius) led to around 4% of the cell-free volume fraction in the particle.

Effect of Substrate Concentration

The effect of the substrate concentration at the surface of the aggregate on the distributions of the steady state cell mass and substrate within the support particles is illustrated in Fig. 3. A higher surface concentration of the substrate led to a deeper cell layer, while a lower substrate concentration amplified the problems of mass transfer resistance. The effectiveness factors for the immobilized cell particles relative to the concentration of the substrate at the surface of the aggregate for 0.5, 1.0, 2.0, and 3 g/L were 0.58, 0.75, 0.93, and 1.00, respectively.

Effect of Inhibition Kinetics

The effect of substrate inhibition on the cell mass concentration is illustrated in Fig. 4. A lower K_I value means a more severe substrate inhibition on cell growth. By equating Eqs. (11) and (17) it was verified that the steady state cell mass concentration was highest at $S = \sqrt{K_I K_s}$. As such, there was a maximum concentration of cell mass inside the particle for $S_0 > \sqrt{K_I K_s}$. The cell mass concentration increased with a decreasing substrate concentration for $\sqrt{K_I K_s} < S < S_0$.

As the K_I value decreased, the cell mass concentration at the surface decreased, while the depth of the cell layer increased. The effectiveness factors based on the substrate consumption rates were 0.76, 0.84, and 0.93 for K_I values of 1.0, 0.15, 0.93, respectively. This indicates that cell growth under diffusional resistance reduced the substrate inhibition effect on the substrate consumption rate.

Next, the effect of product inhibition kinetics on the cell mass concentration are illustrated in Fig. 5. Linearity between the specific substrate consumption rate and the specific product formation rate was used to simplify the calculation of the product concentrations ($\pi/\sigma S$ = 10 $ unit/g substrate). A lower K_p value means a more severe product inhibition on cell growth, as such, a lower K_p value led to a broader distribution of the cell mass concentration and decrease in the product concentration in the particle. The effectiveness factors based on the substrate consumption rates were 0.757, 0.746, and 0.718 for K_p values of 0.667, 0.575, respectively. For the parameters used in these simulations, the accumulation of the inhibitory product slightly decreased the activity of the immobilized cell-support aggregate.

Analytical Solutions with Zero Order Kinetics

The results of the steady state simulations showed

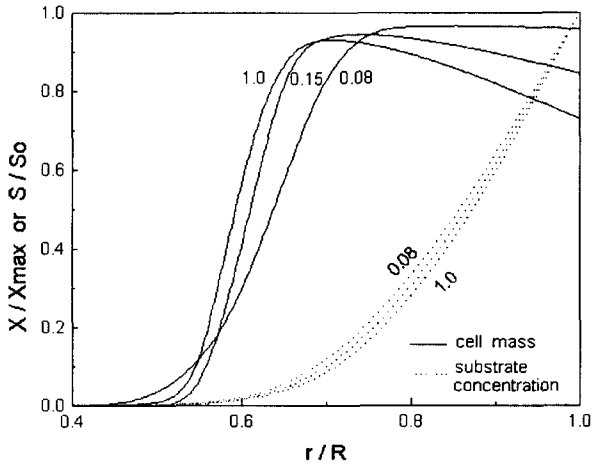

Fig. 4. Effect of substrate inhibition on steady state concentration profiles of cell mass and substrate. The numbers designate the substrate inhibition constant, K_I, in g/L.

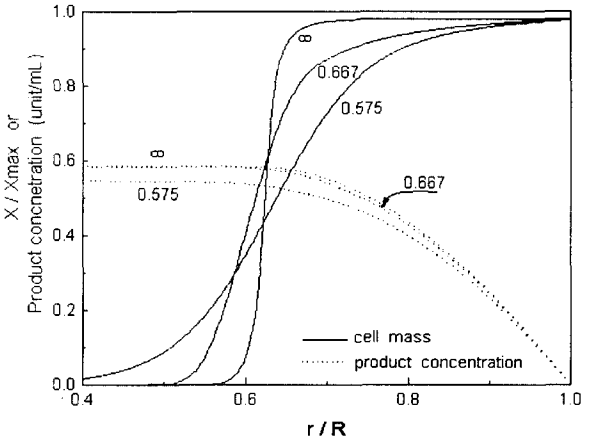

Fig. 5. Effect of product inhibition on steady state concentration profiles of cell mass and product. The numbers designate the P_m value in unit/mL.

the variation in cell mass concentration in a gel bead. The Monod-type cell growth kinetic led to a stiff decline in the cell mass distribution (Fig. 2 and 3), while the inhibition kinetics led to a complicated change, as observed in Figs. 4 and 5. For the short-cut analysis of Monod type kinetics in an immobilized cell bead, a step change in the cell mass concentration was assumed in a steady state. As a result, only the substrate material balance needed to be solved.

$$\frac{1}{r^2}\frac{d}{dr}\left(r^2 D_S \frac{dS}{dr}\right) = \delta_S X \tag{12}$$

The same boundary conditions as in the steady state solution, Eq. (13)-(15), were employed, while the boundary of the living cells was a prior unknown. Further simplification involved an assumption of a zero-order

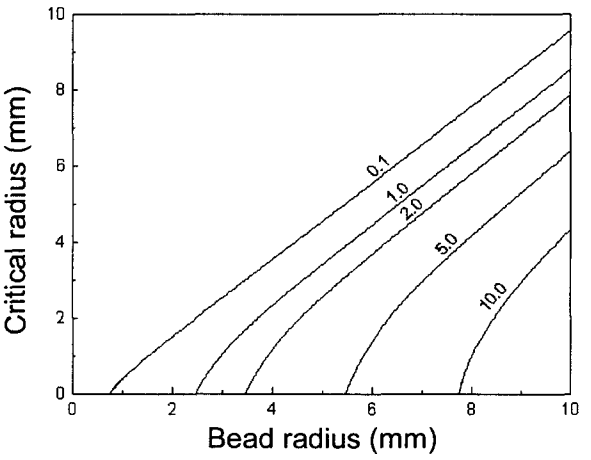

Fig. 6. Critical radius of immobilized cell beads as a function of α as defined in the text. The numbers designate the α value in cm_2.

substrate consumption rate. Since a uniform cell density was assumed, the effective diffusivity was also constant.

This equation was used to analyze the unreacted-core-shrinking spherical particle, and was solved for the core boundary and the distribution of the reactant concentration in the reaction zone [20].

$$S_0 - S(r) = \frac{S_0}{3\alpha}\left[\frac{1}{2}\left(R^2 - r^2\right) + R_c^3\left(\frac{1}{R} - \frac{1}{r}\right)\right] \tag{19}$$

where

$$\alpha \equiv \frac{S_0 D_S}{\delta X_c} \tag{20}$$

A higher value of α indicates a lower mass transfer resistance. The critical radius for the survival of the microorganisms was calculated from the equation, $S(R_c) = 0$. The variation in the critical radius as a function of α and the bead size based on solving the eqn. $S(R_c)=0$, is plotted in Fig. 6.

By defining a dimensionless parameter, θ ($\equiv\alpha/R^2$) , the substrate concentration profiles were calculated in terms of θ (Fig. 7). When the value of θ was over 1/6, the immobilized cell bead had no diffusion limitation. The relation between θ and the critical radius was,

$$\theta = \frac{1}{6}\left(2x^2 - 3x^2 + 1\right) \tag{21}$$

where is the dimensionless critical radius (R_c/R).

While it is very difficult to experimentally confirm substrate profiles in a bead, the average concentration of a substrate through a whole bead can be measured based on the disintegration of the gel beads. The average substrate concentration can be expressed in terms of x and θ.

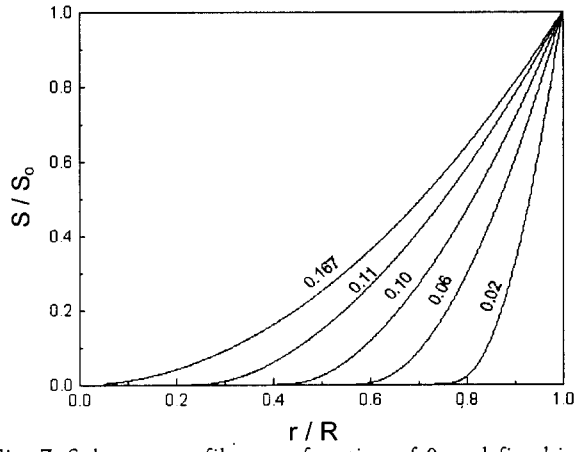

Fig. 7. Substrate profiles as a function of θ as defined in the text. The numbers designate the θ values as defined in the text.

$$\frac{S_{avg}}{S_0} = (1-x^3)\left(1-\frac{1}{6\theta}-\frac{x^3}{3\theta}\right)+\frac{1}{10\theta}(1-x^5)+\frac{x^3}{2\theta}(1-x^2) \quad (22)$$

Effectiveness factor based on substrate consumption is identical to the volume fraction occupied by living cells.

$$\eta = 1 - x^3 \quad (23)$$

The above three relations are plotted in Fig. 8. In this figure the effectiveness factor and the dimensionless parameter, θ, can be estimated from the average substrate concentration. Accordingly, when the average concentration of the substrate was over 60% of the surface concentration, the mass transfer of the substrate did not limit the biocatalyst activity. The relation between θ and the effectiveness factor was also estimated in Fig. 8.

Another application of this plot is the determination of a combined parameter ($D_s/\sigma X_c$). This combined parameter can be estimated from a one-shot experiment by measuring the average substrate concentration of a bead and the substrate concentration in the culture instead of determining each parameter. Once the combined parameter is estimated, the effectiveness factor at various substrate concentrations and bead diameters can be predicted.

The effectiveness factors estimated from the average substrate concentrations were compared with the results of rigorous steady state simulations (Figs. 2-5). As given in Fig. 9, the effectiveness factors for the Monod-type kinetics (high K_I value of 1,000) were in good agreement with the results of the zero-order approximation, while the substrate inhibition kinetics and product inhibition kinetics exhibited a discrepancy due to an extremely non-uniform cell distribution. The effectiveness factor for the substrate inhibition kinetics was higher than that for the Monod-type kinetics because the mass concentration at the surface was lower

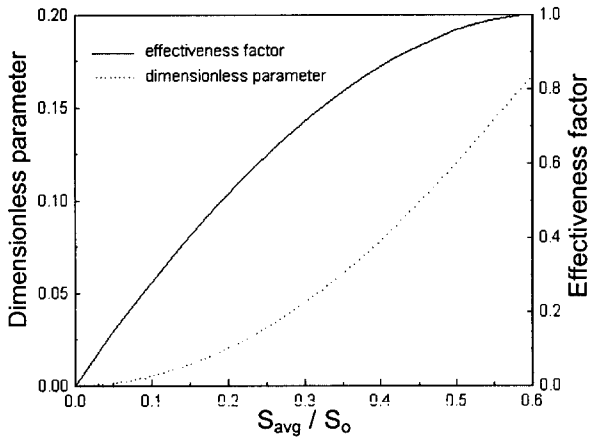

Fig. 8. Relation between dimensionless parameter (θ), effectiveness factor, and average substrate concentration.

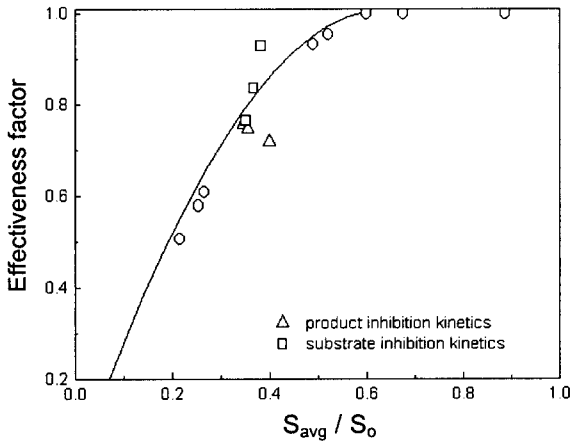

Fig. 9. Effectiveness factor as a function of the average substrate concentration.

than inside the bead, whereas the product inhibition kinetics produced the opposite trend, that is, a lower effectiveness factor than that for the Monod-type kinetics.

CONCLUSION

The mathematical model discussed in this study is capable of predicting steady state and transient concentration profiles of the cell mass and substrate in an immobilized cell-support aggregate. The model was employed to study the effects of particle size and substrate concentration at the surface of the particle. As anticipated, a smaller bead size and higher substrate concentration at the surface of the particle resulted in more of the substrate being supplied into the aggregate and consequently a higher biocatalyst activity.

The model developed in this study can be employed in the analysis of an immobilized cell reactor. The de-

velopment of a mathematical model for the overall immobilized cell process can be significantly simplified in well-mixed continuous flow bioreactors if all aggregates are considered as having (i) the same size, and (ii) the same cell mass distribution and identical surface conditions.

The overall mathematical model is comprised of material balance equations for the cell mass, major carbon source, dissolved oxygen, and non-biomass products in a bulk (mobile) suspension plus the single particle model proposed in this study. The biomass balance in the bulk (gel bead-free) suspension should also account for any cell leakage from the support particles into the bulk suspension.

NOMENCLATURE

D_i : effective diffusivity of species i, i = S, P, G [cm^2/h]
G : co-substrate (oxygen) concentration [g/L]
k : endogenous metabolism or cell death rate [h^{-1}]
K_I : substrate inhibition constant [g/L]
K_P : product inhibition constant [g/L]
m_s : specific substrate consumption rate for maintenance [g substrate/g cell/h]
P : product concentration [unit/mL]
r : radial position in bead [cm]
R : radius of bead [cm]
S : substrate concentration [g/L]
t : time [h]
X : cell mass concentration [g dry cell/L]
$Y_{x/s}$: cell mass fraction [g cell/g substrate]

Greek Symbols

η : effectiveness factor
θ : dimensionless parameter ($\equiv \alpha/R^2$)
μ : specific cell growth rate [g/L]
π : specific product formation rate [h^{-1}]
ρ_X : dry cell weight per unit volume of active cells [g dry cell/L active cell]
σ : specific substrate consumption rate [h^{-1}]
ϕ_C : cell volume fraction
x : dimensionless critical radius

Subscripts

avg : average
c : critical
e : effective
free : in suspension culture
G : co-substrate
m : maximum
0 : initial
s : substrate

REFERENCES

[1] Gikas, P. and A. G. Livingston (1997) Specific ATP and specific oxygen uptake rate in immobilized cell aggregates: experimental results and theoretical analysis using a structured model of immobilized cell growth. *Biotechnol. Bioeng.* 55: 660-673.
[2] Monbouquette, H. G., G. D. Sayles, and D. F. Ollis (1990) Immobilized cell biocatalyst activation and pseudo-steady-state behavior, model and experiment. *Biotechnol. Bioeng.* 35: 609-629.
[3] Riley, M. R., F. J. Muzzio, and S. C. Reyes (1997) Effect of oxygen limitations on monoclonal antibody production by immobilized hybridoma cells. *Biotechnol. Prog.* 13: 301-310.
[4] Nakasaki, K., T. Murai, and T. Akiyama (1989) Dynamic modeling of an immobilized cell reactor. *Appl. Biochem. Bioeng.* 22: 279-288.
[5] Godia, F., C. Casas, and C. Sola (1987) Mathematical modelization of a packed-bed reactor performance with Immobilized yeast for ethanol fermentation. *Biotechnol. Bioeng.* 30: 836-843.
[5] Berry, F., S. Sayadi, M. Nasri, J. N. Barbotin, and D. Thomas (1988) Effect of growing conditions of recombinant *E. coli* in carrageenan gel beads upon biomass production and plasmid stability. *Biotechnol. Lett.* 10: 619-624.
[6] Sola, C., C. Casas, M. Poch, and A. Serra (1986) Continuous ethanol production by immobilized yeast cells and ethanol recovery by liquid-liquid extraction. *Biotechnol. Bioeng Symp.* No.17: 519-533.
[7] du Poet, P. T., P. Dhulster, J. N. Barbotin, and D. Thomas (1986) Plasmid inheritability and biomass production, comparison between free and immobilized cell cultures of *Escherichia coli* BZ18(pTG201) without selection pressure. *J. Bacteriol.*165: 871-877.
[8] Wang, H., M. Seki, and S. Furusaki (1995) Mathematical model for analysis of mass transfer for immobilized cells in lactic acid fermentation. *Biotechnol. Prog.* 11: 558-564.
[9] Tsuchiya, K. and T. Kimura (1980) Growth kinetics under adenine limiting conditions of KYA 741, and adenine-requiring strain. *Biotechnol. Bioeng.* 22: 401-410.
[10] Konak, A. R (1975) An equation for batch bacterial growth. *Biotechnol. Bioeng.* 17: 271-272.
[11] Tayeb, Y. J. and H. C. Lim (1986) Optimal glucose feed rate for fed-batch penicillin fermentation, an efficient algorithm and computational results. *Ann. N.Y. Acad. Sci.* 469: 382-403.
[12] Chresand, T. J., B. E. Dale, and S. L. Hanson (1988) A stirred bath technique for diffusivity measurement in cell matrices. *Biotechnol. Bioeng.* 32: 1029-1036.
[13] Zhao, Y. and G. B. DeLancey (2000) A diffusion model and optimal cell loading for immobilized cell biocatalysts. *Biotechnol. Bioeng.* 69: 639-647.
[14] Johnson, M. J (1967) Aerobic microbial growth at low oxygen concentrations *J. Bacteriol.* 94: 101-108.
[15] Chen, T.-L. and A. E. Humphrey (1988) Estimation of critical particle diameters for optimal respiration of gel entrapped and/or pelletized microbial cells. *Biotechnol. Lett.* 10: 699-702.
[16] Khang, Y. H., H. Shankar, and F. Senatore (1988) Modelling the effect of oxygen mass transfer on β-lactam antibiotics production by immobilized *Cephalosporium acremonium*. *Biotechnol. Lett.* 10: 861-866.

[17] Bajpai, R. K. and M. Reuss (1980) A mechanistic model for penicillin production. *J. Chem. Tech. Biotechnol.* 30: 332-344.
[18] Davis, M. E. and L. J. Watson (1985) Analysis of a diffusion-limited hollow fiber reactor for the measurement of effective substrate diffusivities. *Biotechnol. Bioeng.* 27: 182-186.
[19] McGinnis, P. H. Jr (1965) Numerical solution of boundary value nonlinear ordinary differential equations. *Chem. Eng. Prog. Symp. Ser.* 61: 2-7.
[20] Wen, C. Y (1968) Noncatalytic heterogeneous solid fluid reaction models. *Ind. Eng. Chem.* 60: 34-54.

[Received December 1, 2000; accepted January 27, 2001]